

## Supporting Information to

# **Nitrogen-doped Porous Carbon Networks with Active Fe-N<sub>x</sub> Sites to Enhance Catalytic Conversion of Polysulfides in Lithium-Sulfur Batteries**

He Yang, Yanan Yang, Xu Zhang,\* Yongpeng Li, Naeem Akhtar Qaisrani, Fengxiang Zhang\* and Ce Hao

State Key Laboratory of Fine Chemicals, School of Petroleum & Chemical Engineering, Dalian University of Technology, Panjin 124221, China

\* Corresponding author; E-mail: zhangfx@dlut.edu.cn; zhangxu@dlut.edu.cn

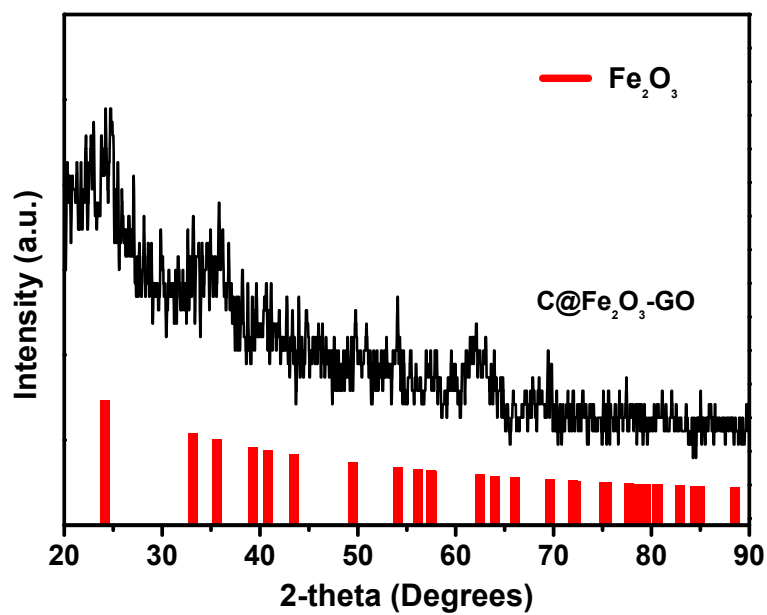


**Figure S1.** XRD patterns of C@Fe<sub>2</sub>O<sub>3</sub>-GO.

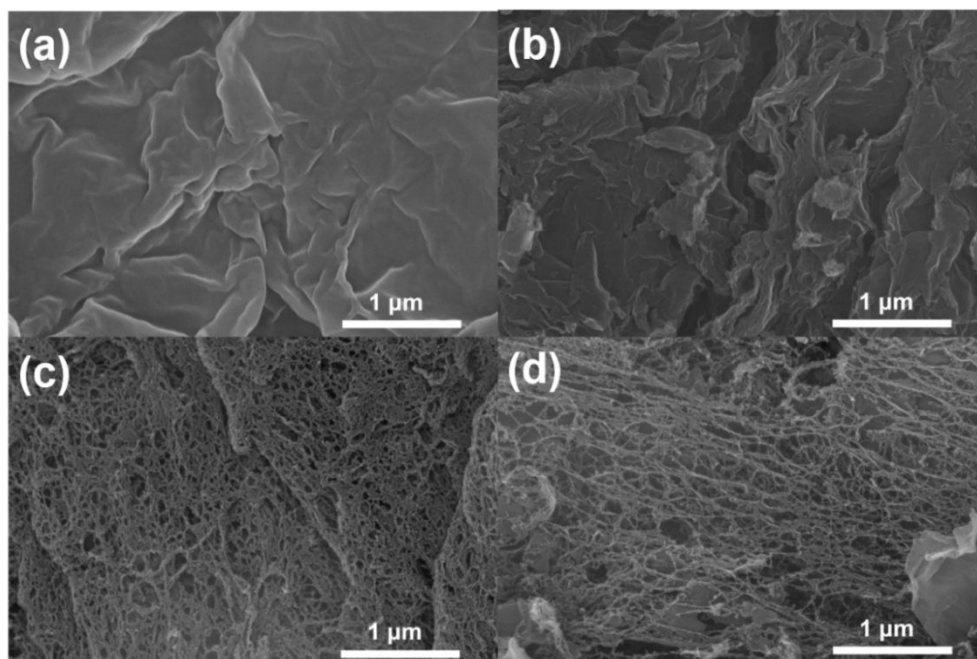


**Figure S2.** SEM images of (a) C@Fe<sub>2</sub>O<sub>3</sub>-GO, (b) Fe<sub>3</sub>C@C, (c) Fe<sub>3</sub>C/Fe-N<sub>x</sub>@NPCN, and (d) NPC.

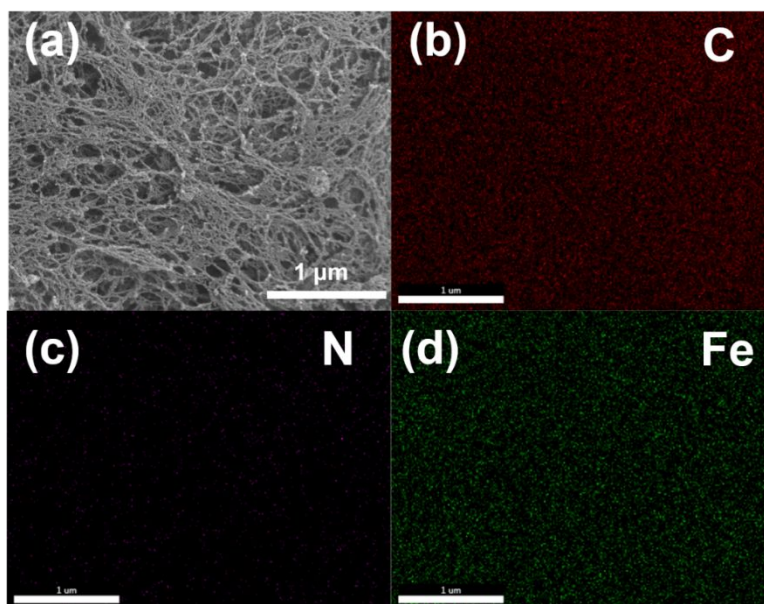


**Figure S3.** (a) SEM image of  $\text{Fe}_3\text{C}/\text{Fe-N}_x@\text{NPCN}$ , and the corresponding elemental mapping of (b) C; (c) N; (d) Fe.

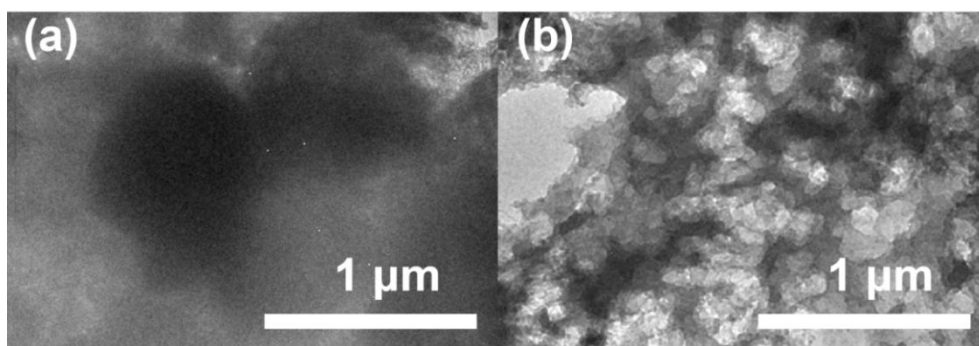


**Figure S4.** TEM images of (a)  $\text{Fe}_3\text{C}@\text{C}$ ; (b) NPC.

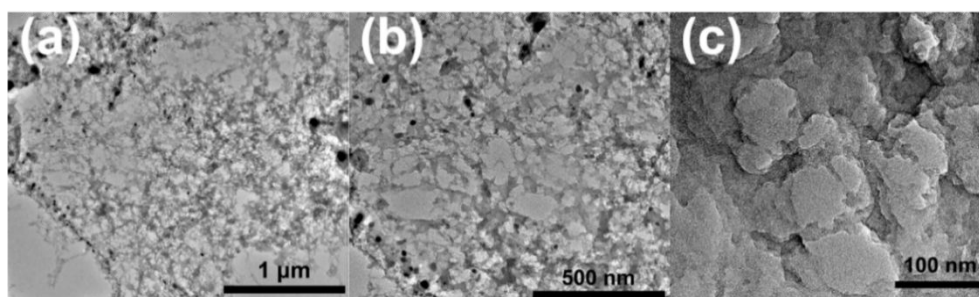


**Figure S5.** TEM images of  $\text{Fe}_3\text{C}/\text{Fe-N}_x@\text{NPCN}$ .

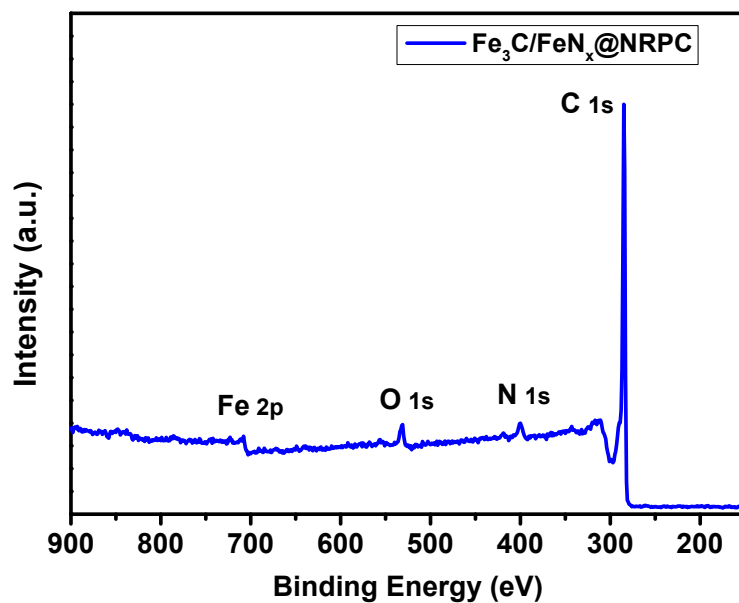


Figure S6. Wide scan XPS spectrum of  $\text{Fe}_3\text{C}/\text{Fe-N}_x@\text{NPCN}$ .

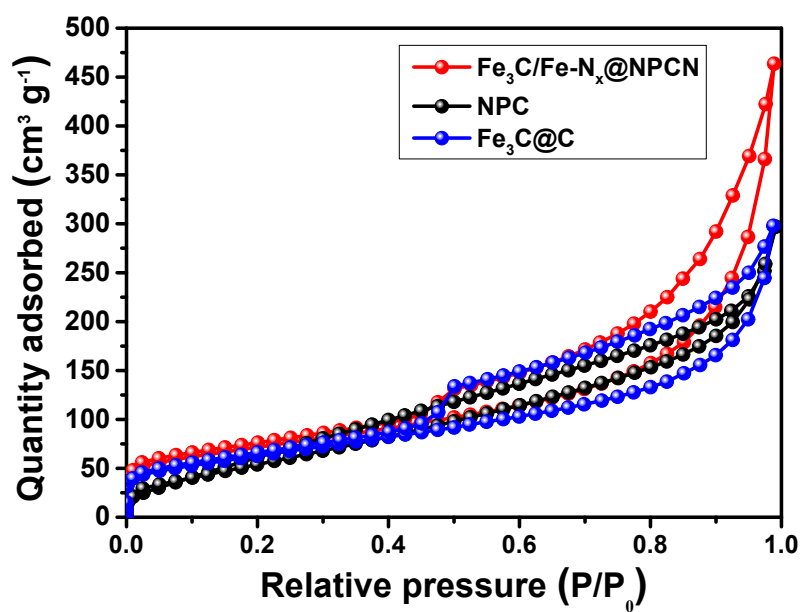


Figure S7.  $\text{N}_2$  adsorption-desorption isotherms of  $\text{Fe}_3\text{C}/\text{Fe-N}_x@\text{NPCN}$ ,  $\text{Fe}_3\text{C}@\text{C}$  and NPC composites.

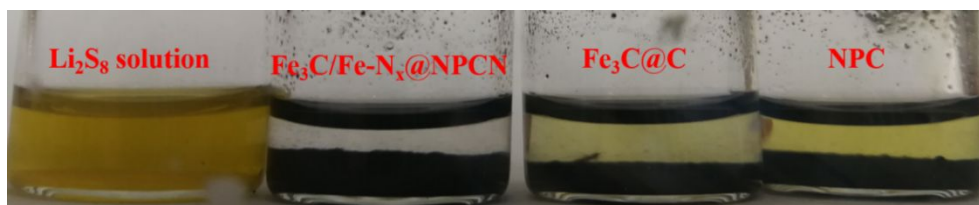
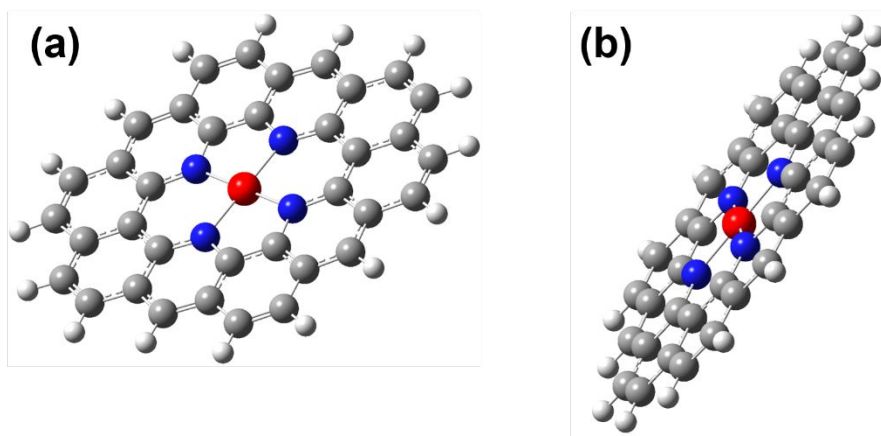
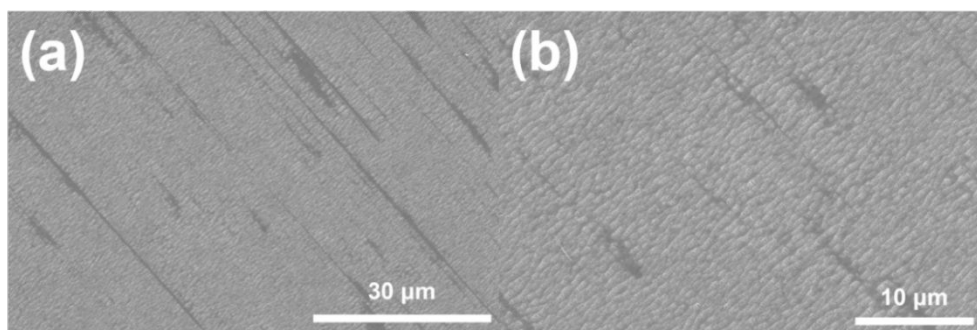


Figure S8. Digital image of the  $\text{Li}_2\text{S}_8$  (0.05 M) solution after soaking  $\text{Fe}_3\text{C}/\text{Fe-N}_x@\text{NPCN}$ ,  $\text{Fe}_3\text{C}@\text{C}$  and NPC for 30 min.



**Figure S9.** Structures of Fe-N<sub>4</sub> moieties on N-doped porous carbon networks used in first-principles calculations.



**Figure S10.** SEM images of pure PP membrane under different magnifications.

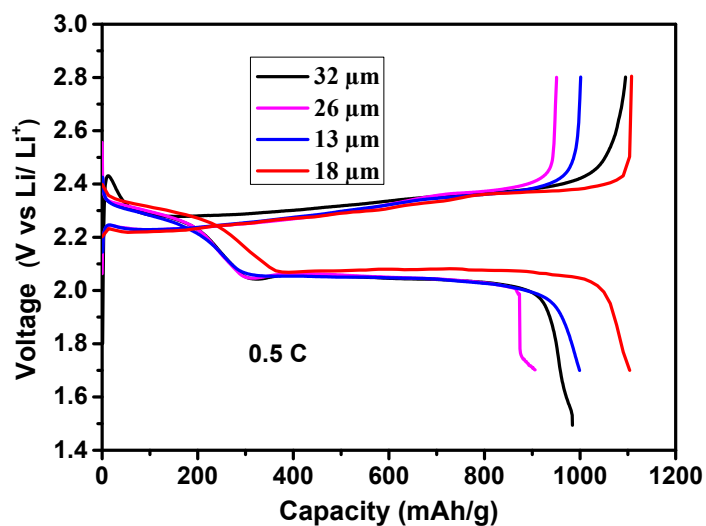


**Figure S11.** Discharge curves of the Li-S batteries assembled with modified PP separators of different Fe<sub>3</sub>C / Fe-N<sub>x</sub>@NPCN coating thickness values.

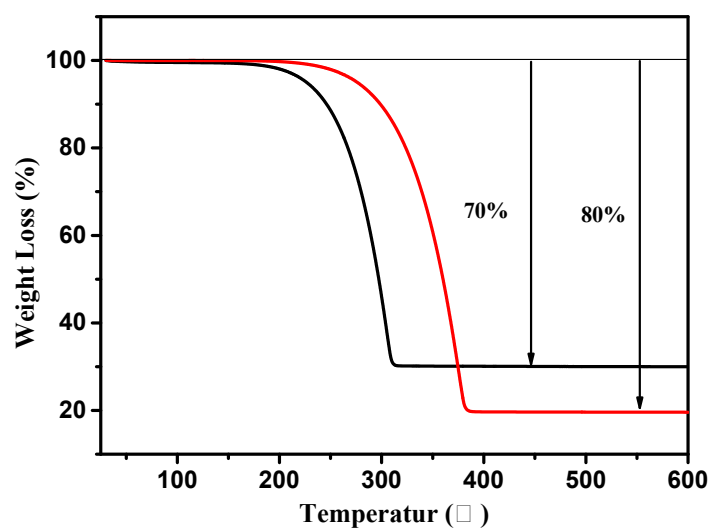


**Figure S12.** TGA of super-P/S under N<sub>2</sub> atmosphere.

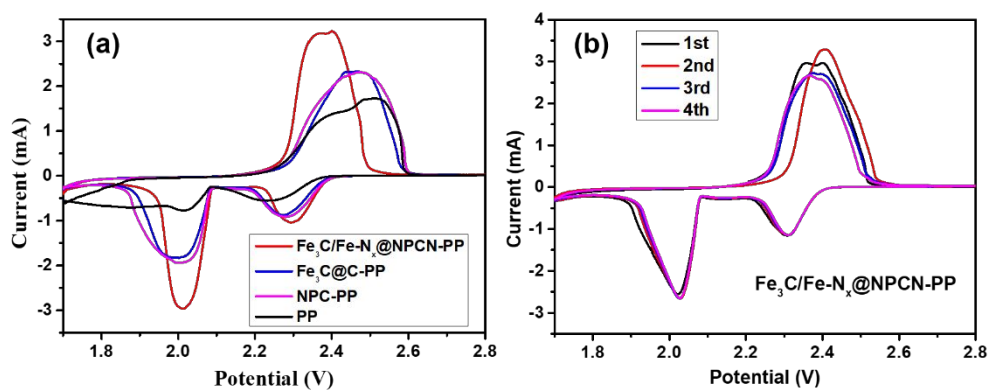


**Figure S13.** CV profiles of (a) Fe<sub>3</sub>C/Fe-N<sub>x</sub>@NPCN-PP, Fe<sub>3</sub>C@C-PP, NPC-PP, and PP batteries. (b) CV profiles of Fe<sub>3</sub>C/Fe-N<sub>x</sub>@NPCN-PP at different cycles.

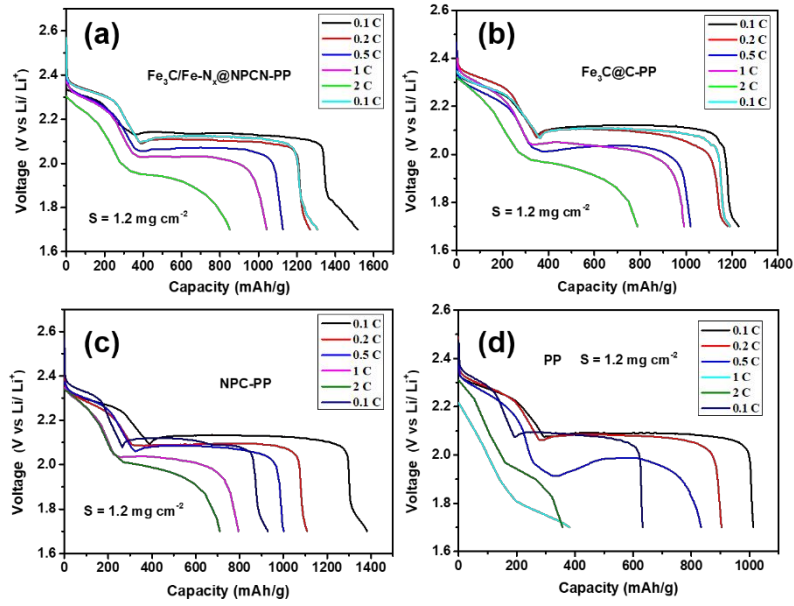


**Figure S14.** (a-d)  $\text{Fe}_3\text{C}/\text{Fe-N}_x@\text{NPCN-PP}$ ,  $\text{Fe}_3\text{C}@\text{C-PP}$ , NPC-PP and PP batteries galvanostatic discharge-charge profiles at 0.1 to 2 C.

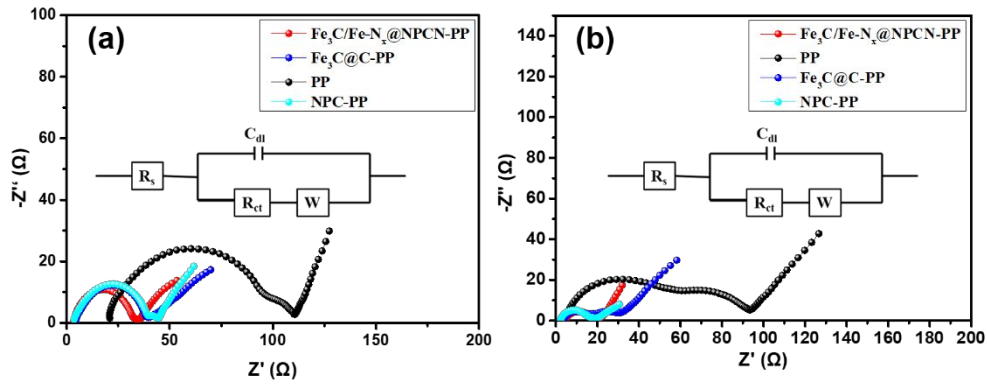


**Figure S15.** Nyquist plots of the  $\text{Fe}_3\text{C}/\text{Fe-N}_x@\text{NPCN-PP}$ ,  $\text{Fe}_3\text{C}@\text{C-PP}$ , NPC-PP and PP batteries (a) before cycling and (b) after 50 cycles at 0.5 C.

**Table S1.** Physical properties of PP separator.

Thickness	JIS Gurley	TD Shrinkage	Pore size
25 $\mu\text{m}$	620 seconds	0%	0.028 $\mu\text{m}$